Core−Shell Nanoporous Electrode for Dye Sensitized Solar Cells: the Effect of the $SrTiO_3$ Shell on the Electronic Properties of the TiO_2 Core

Yishay Diamant, S. G. Chen, Ophira Melamed, and Arie Zaban*

Department of Chemistry, Bar-Ilan University, Ramat-Gan, 52900 Israel

Received: December 25, 2002

A nanoporous TiO_2 electrode coated with a thin $SrTiO_3$ layer was synthesized for photoelectrochemical applications. Introduction of this core−shell electrode to a dye sensitized solar cell increased the open circuit photovoltage while reducing the short circuit photocurrent in comparison with a cell containing the standard noncoated TiO_2 electrode. The photovoltage increases is more significant than the photocurrent reduction resulting in a 15% improvement of the overall conversion efficiency of the solar cell. The performance of the TiO_2−$SrTiO_3$ core−shell electrode in the dye sensitized solar cell was analyzed by several methods including photocurrent−voltage correlation, spectro-electrochemistry, dark current measurement, IPCE, and photovoltage spectroscopy. The results indicate that the $SrTiO_3$ layer shifts the conduction band of the TiO_2 in the negative direction rather than forming energy barrier at the TiO_2/electrolyte interface as found for similar coating by other materials. The shift of the TiO_2 bands is attributed to a surface dipole that is induced by the $SrTiO_3$ coating.

Introduction

Since the introduction of the nanoporous electrode, dye sensitized solar cells (DSSCs) have become a low cost efficient alternative to the conventional silicon cells.[1,2] The high surface area of the nanoporous electrode enables both efficient light harvesting and electron injection by a dye monolayer in contrast to the compact electrode in which high optical density can be achieved only with several dye layers which have poor electron injection efficiency.[3−6] The highest efficiency of DSSCs (11%) was achieved for cells utilizing TiO_2 as the nanoporous material.[1,7] However, these cells still suffer from a high recombination rate between the injected electrons and the oxidized dye or ions in solution. The high recombination rate in DSSCs is attributed to the small size of the particles, which cannot establish significant band banding.[8−10] That is, an electric field that spatially separates the injected electrons from the holes in the dye or solution is not formed at the electrode−electrolyte interface. Consequently, the large electrode−electrolyte interface area enables high recombination currents.[8,11] Two basic approaches to overcome this loss mechanism were suggested. One involves the formation of an isolating layer at the exposed electrode surface.[12−16] In the other method, an energy barrier that allows electron injection but stops the recombination reaction is fabricated at the nanoporous electrode surface.[17−26] Both approaches showed promising results.

In previous studies, we reported the fabrication of such an energy barrier on nanoporous TiO_2 electrodes.[26] The barrier was made by a thin Nb_2O_5 coat whose conduction band potential is 100 mV negative than that of the TiO_2. The Nb_2O_5 barrier layer restricts the electrons to the TiO_2 particles, thus reducing the recombination rate.[26] Consequently, all parameters of the DSSC improved resulting in a 35% increase of the cell efficiency.[22,26] Figure 1 shows a schematic view of the Nb_2O_5/TiO_2 core−shell electrode and its superiority regarding recombination.

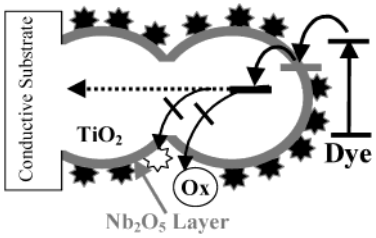

Figure 1. Schematic view of the Nb_2O_5/TiO_2 core−shell electrode. The Nb_2O_5 layer, having a conduction band more negative than that of TiO_2, forms an energy barrier at the TiO_2 surface, thus, reducing the recombination rate.

Based on the Nb_2O_5/TiO_2 core−shell experience, we expected that similar electrode which is based on a semiconductor whose conduction band is higher than that of the Nb_2O_5 will exhibit even higher performance. Such properties are available for $SrTiO_3$ that should form a 200 mV barrier on TiO_2 based on the conduction band difference between these materials.[27,28] Furthermore, based on the matching between the unit cell parameters, it is reasonable to assume an epitaxial growth between parallel plans in the square facet of the TiO_2 tetragonal unit cell and the $SrTiO_3$ cubic unit cell.

In this work, we report the synthesis of a $SrTiO_3$ coated nanoporous TiO_2 electrode and its effect on the performance of DSSCs. The coated nanoporous electrode was examined by means of current voltage dependence (i−V) of the solar cell when illuminated and in the dark, incident photon to current efficiency (IPCE), spectro-electrochemistry, and photovoltage spectroscopy. The results indicate that, unlike the Nb_2O_5 that forms an energy barrier at the surface, the $SrTiO_3$ coating shifts the conduction band of the TiO_2 in the negative direction showing no surface energy barrier formation. The conduction band shift increases the open circuit voltage (Voc) of the DSSC while decreasing the short circuit current (Jsc). The Voc increase is more significant than the loss of current; thus, the overall efficiency of the cell increased by 15.3% because of the $SrTiO_3$ coating.

* To whom correspondence should be addressed. E-mail: zabana@mail.biu.ac.il.

10.1021/jp027827v CCC: $25.00
Published on Web 02/11/2003

Experimental Section

Film Preparation. TiO_2 colloids were prepared by hydrolysis of 1:1 solution of titanium (IV) isopropoxide (Aldrich, 99.9%) and 2-propanol in acetic acid (pH = 2). After overnight aging, the organic remainders were evaporated at 82 °C followed by a hydrothermal treatment at 250 °C for 13 h (titanium autoclave, Parr). The production of the TiO_2 slurry was completed by sonication for 5 min, addition of Carbowax (poly(ethylene glycol) compound) to solution, and stirring overnight. Using TEM and XRD, the TiO_2 particles were characterized as 23 nm in diameter anatase crystals. The TiO_2 slurry was spread on conducting glass substrates (Hartford glass, 8 ohm/square F-doped SnO_2) using adhesive tapes as spacers. The films were dried in air at room temperature and sintered at 450 °C for 30 min. The thickness of the TiO_2 films was 4 μm, measured with Surftest SV 500 profilometer (Mitutoyo Co).

The $SrTiO_3$ coating of the nanoporous TiO_2 electrode was fabricated by dip coating in ethanol solution containing strontium precursors. Three precursors at various concentrations were studied: strontium oxide (99.9%), strontium isopropoxide (99.9%), and strontium chloride (99.99%). All three precursors were purchased from Aldrich Chemical Co. and used as received. After the dipping, the electrode was washed with dry ethanol and sintered again at 550 °C for 30 min.

Sensitization of the electrodes was done by overnight immersion in dry ethanol solution containing 0.5 mM of the N3 dye (*cis*-di(isothiocyanato)-*N*-bis(4,4′-dicarboxy-2,2′-bipyridine) ruthenium(2)) (Solaronix SA). To prevent hydration, the electrodes were heated to 150 °C and cooled to 80 °C before dipping in the dye solution.

Electrochemical and Photoelectrochemical Measurements. The solar cell performance was measured in a sandwich-type configuration using Pt coated conductive glass as a counter electrode. The electrolyte solution consisted of 0.5 M LiI/0.05 M I_2 in 1:1 acetonitrile-NMO (3-methyl-2-oxazolidinone). A 250 W xenon lamp, calibrated to 1 sun in the visible range, served as a light source.

The dark current measurements were done using nanoporous electrodes that were treated to block the exposed area of the conducting glass substrate. The electrochemical blocking by the isolating polyphenoxide was done before immersion in the dye solution, utilizing a published procedure.[16]

Spectro-electrochemical measurements were conducted by incorporating the studied electrode as a working electrode in a three-electrode Teflon cell. The counter and the reference electrodes were a platinum wire and Ag/AgCl, respectively. The electrolyte consisted of pH 1.8 $HClO_4$ solution, with 0.2 M $LiClO_4$ as supporting electrolyte. To avoid oxygen, the solution was bubbled with nitrogen for 30 min before the experiments.

All electrochemical measurements were performed using an Eco Chemie Autolab 20 potentiostat.

Results and Discussion

The effect of the $SrTiO_3$ coating on the properties of the nanoporous electrode were measured and analyzed in a comparative mode. All measurements involved a $SrTiO_3$ coated TiO_2 electrode and a reference bare TiO_2 electrode made in the following way. A nanoporous TiO_2 electrode was prepared and cut into two identical pieces. One of the two electrodes was coated with $SrTiO_3$ and sintered a second time. The reference bare TiO_2 electrode was also sintered a second time together with the $SrTiO_3$ coated TiO_2 electrode to ensure similarity. The two reported electrodes, bare TiO_2 and $SrTiO_3$ coated TiO_2, had similar thickness and appearance. Absorption spectra of the dyed electrodes indicate equal amounts of adsorbed dye.

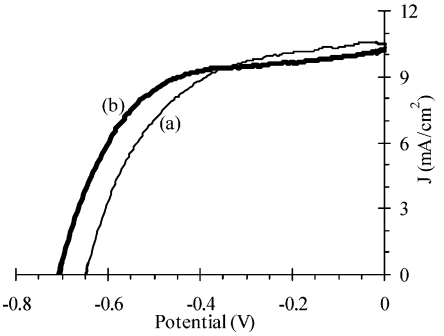

Figure 2. *i*−*V* curves of DSSCs which consist of the (a) bare TiO_2 and (b) $SrTiO_3$ coated TiO_2 electrodes.

TABLE 1: Performance Comparison of the DSSCs Consisting of the Bare TiO_2 and $SrTiO_3$ Coated TiO_2 Electrodes under a Xe Source 1 Sun Simulator. The Measurement Conditions of Both Electrodes Were Similar. Cell Area Was 0.6 cm^2

electrode	Voc (mV)	Jsc (mA/cm^2)	fill factor (%)	eficiency (%)
bare TiO_2	650	10.5	53.6	3.81
$SrTiO_3$ coated TiO_2	708	10.2	58.4	4.39

Several precursors at different concentrations and dipping duration were tested. In addition, the sintering temperature and duration were varied. The largest effect was observed for dipping of the TiO_2 electrode in strontium oxide solution for 45 s followed by 30 min sintering at 550 °C. Therefore, the results discussed below relate to this coating procedure. It is important to note that we confirm by XPS measurements the existence of strontium throughout the nanoporous TiO_2 film. However, the exact structure of the strontium coating layer and its uniformity are not clear. We consider this ambiguity in the interpretation of the $SrTiO_3$ coating results presented below.

Figure 2 shows the photocurrent−voltage dependences (i−V curves) of DSSCs that consist of the $SrTiO_3$ coated TiO_2 and bare TiO_2 electrodes. The corresponding solar cell parameters are summarized in Table 1. Compared with bare TiO_2, the $SrTiO_3$ coating increased the open circuit photovoltage (Voc) from 650 to 708 mV, and the fill factor increased from 53.6 to 58.4%. However, the short circuit photocurrent (Jsc) decreased from 10.5 to 10.2 mA/cm^2 because of the coating. As a result, the overall conversion efficiency increased by 15.3% from 3.81 to 4.39%.

The $SrTiO_3$ coating effect on the DSSC performance is significantly different from the Nb_2O_5 coating of TiO_2 that triggered this study. In the case of Nb_2O_5 coating, all cell parameters, i.e., Voc, Jsc, and the fill factor, increased. In ref 22, we showed that the improvement of all cell parameters results from the energetic barrier formed by the Nb_2O_5 at the TiO_2 surface. In other words, the reduction of the recombination rate in the solar cell by this energy barrier increases the electron concentration at Voc and the electron collection efficiently throughout the voltage scan. In the case of $SrTiO_3$ where the photovoltage increases is coupled with a decrease of the photocurrent, two possible mechanisms should be examined. In one mechanism, the $SrTiO_3$ layer forms an energy barrier at the electrode surface thus reducing the recombination current. However, at the same time, this barrier reduces the electron injection efficiency thus decreasing the cell's photocurrent. Less efficient injection can result from the relatively negative conduction band potential of the $SrTiO_3$ or from the dye-

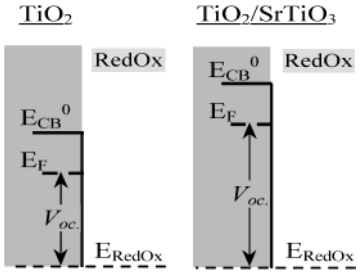

Figure 3. Energy diagram representing the movement of the TiO_2 conduction band by the $SrTiO_3$ coating and its effect on the measured photovoltage.

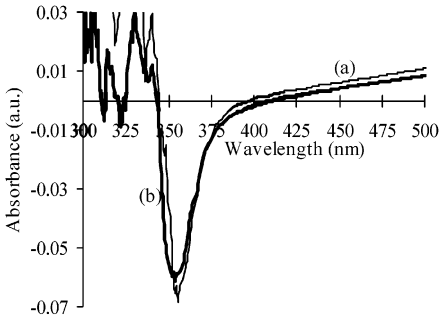

Figure 4. Spectral changes of the (a) bare TiO_2 and (b) $SrTiO_3$ coated TiO_2 electrodes at applied −0.9 V vs SCE in $HClO_4$ aqueous solution (pH 1.8). The short wavelength bleach that is related to the electrons accumulation in the TiO_2 is not effected by the coating.

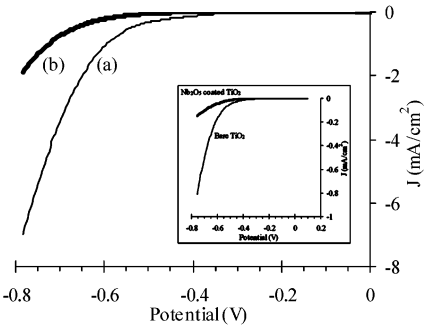

Figure 5. Dark current measurement of the (a) bare TiO_2 and (b) $SrTiO_3$ coated TiO_2 electrodes in the DSSCs presented in Figure 2. The inset shows the effect of Nb_2O_5 coating compare to bare TiO_2.

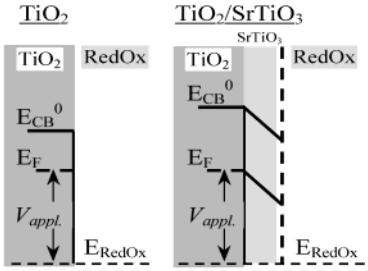

Figure 6. Energy diagram showing the effect of the band shift on the nanoporous electrode conductivity. The position of the conduction band relative to the Fermi level which is adjusted by the applied potential indicates that at any applied potential the coated system is more resistive than the bare one.

semiconductor coupling quality.[27,28] In the other possible mechanism, the $SrTiO_3$ does not form an energy barrier, and the effect is mainly a negative shift of the TiO_2 conduction band induced by the coating. This possibility is supported by previous reports in which a shift of the TiO_2 bands negatively resulted in changes similar to those presented in Figure 3.[29−31] On the basis of the results presented below, we find that the second option, i.e., a negative shift of the TiO_2 conduction band potential, describes the $SrTiO_3$ coating better.

Spectro-Electrochemical Experiments. Spectral changes of the nanoporous electrodes under applied potentials that are more negative than the open circuits potential (OCV) are attributed to accumulation of free electrons in the conduction band of the TiO_2.[32,33] Figure 4 presents the absorbance-change spectra of $SrTiO_3$-coated TiO_2 and bare TiO_2 electrodes induced by applying −0.8 V vs Ag/AgCl. The spectral changes measured in $HClO_4$ aqueous solution (pH 1.8) refer to the OCV baseline spectrum. The spectra may be divided to two regions below and above the band gap energy, approximately 400 nm. At wavelengths longer than 400 nm, the intensity increases because of the absorbance of free electrons in the electrode. Below 400 nm, a bleaching peak appears because of an increase of the excitation energy from the valance band to the lowest states of the conduction band that are not filled by the electrochemical process. In other words, the width of the bleaching peak can be related to the electron accumulation in the semiconductor. The bleaching below 400 nm shown in Figure 4 is identical for both the reference and the $SrTiO_3$ coated electrodes, which indicates that the coating does not effect the accumulation of electrochemically injected electrons. In other words, the $SrTiO_3$ does not form an efficient energy barrier. We note that in the case of Nb_2O_5 coating the formation of an energy barrier induced widening of the bleaching peak.[22]

Dark Current Measurement. The dark current of DSSCs does not simulate the recombination current under illumination. The main reason relates to local electrolyte concentration (inside the porous) and to the potential distribution across the nanoporous TiO_2 electrode that is significantly different under illumination compared with dark conditions.[34] However, the dark current can be used to measure a conduction band shift or the existence of an energy barrier at the electrode surface. Like spectroelectrochemistry, this measurement does not involve electron injection from the dye thus eliminating the possibility that the observation results from a change in the injection efficiency through the $SrTiO_3$ coating. To eliminate the effect of the conductive substrate, an isolating layer of polyphenoxide was deposited on the exposed surface of the conducting glass.[16] Blocking of the free surface of the conductive substrate ensures that we test changes at the nanoporous semiconductor only. Figure 5 presents the dark current of the $SrTiO_3$ coated and bare TiO_2 electrodes in the cells presented in Figure 2. The curves have the same shape, whereas the $SrTiO_3$ coating induces a shift of the curve to negative potentials. The shape similarity indicates that the $SrTiO_3$ coating does not reduce the dark current as observed in the case of Nb_2O_5 coating (see inset in Figure 5). In this case, it seems that the observed phenomena should be related to an increase of the TiO_2 resistance resulting from the negative shift of its conduction band. At each applied potential, the electron concentration in the coated TiO_2 is lower than in the bare TiO_2 which reduces the effective area of the nanoporous electrode.[34] Consequently, similar to the spectroelectrochemical measurements, the dark currents indicate that the $SrTiO_3$ coating does not form an efficient energy barrier at the TiO_2 surface (Figure 6).

Collection Efficiency. A comparison between the incident photon to current efficiency (IPCE) of the coated and the bare electrodes can reveal a coating effect on the collection efficiency. The recombination process is wavelength dependent because the penetration length of the light increases with the decreases of the absorption coefficient of the dye. In other words, illumination at wavelengths in which the dye absorption

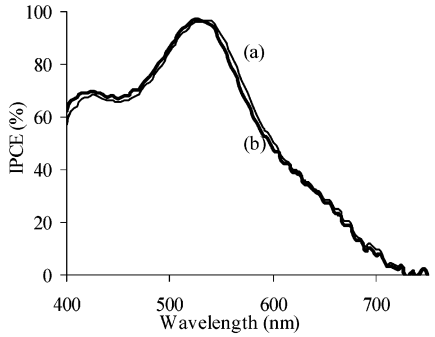

Figure 7. Incident photon to current efficiency (IPCE) of the solar cells consisting of the (a) bare TiO_2 and (b) $SrTiO_3$ coated TiO_2 electrodes, normalized to 100% at the peak value. The similarity indicates that the electrons collection efficiency is not improved by the coating.

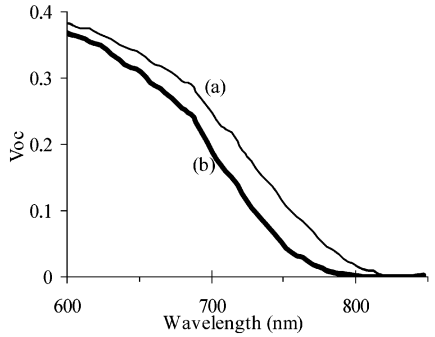

Figure 8. Open circuit photovoltage as a function of the illumination wavelength for DSSCs containing the (a) bare TiO_2 and (b) $SrTiO_3$ coated TiO_2 electrodes. The $SrTiO_3$ coating shifts the onset of injection to shorter wavelength, indicating the movement of the TiO_2 conduction band with respect to the dye oxidation potential.

coefficient is low leads to the photoinjection of electrons a long way from the current collector. If such a distance is longer than the electron diffusion length, these electrons are lost in recombination processes. For example, in the case of the Nb_2O_5 coating where the recombination rate is reduced, higher IPCE values are measured at wavelengths of low dye absorbance. Figure 7 presents the normalized IPCE of two cells consisting of the bare and the coated electrodes. The shapes of the two IPCE curves are similar, meaning that the $SrTiO_3$ coating does not affect the collection efficiency. That is, regardless of the exact efficiency of electron injection across the coating layer. Figure 7 shows that an energy barrier that reduces the recombination rate is not formed by the $SrTiO_3$.

On-Set of Injection. The relative position between the ground state of the dye and the TiO_2 conduction band can be extracted from a correlation between the open circuit photovoltage and the illumination wavelength. Electron injection and thus photovoltage occur when the illumination energy is sufficient for excitation of the electron in the dye to the lowest dye excited state that is located above the conduction band edge. Because the onset of injection usually occurs at wavelength region of low dye absorption, the photovoltage that depends exponentially on the light intensity is much more sensitive to injection than the photocurrent that has a linear dependence. Figure 8 presents the open circuit photovoltage of the $SrTiO_3$-coated and bare TiO_2 electrodes as a function of the illumination wavelength, scanning from long wavelength downward. The injection onset shifts to shorter wavelength upon the $SrTiO_3$ coating of the TiO_2 electrode, indicating a negative movement of the conduction band of the TiO_2 with respect to the dye ground state. This finding correlates with the white light measurements of the solar cell (Figure 2). On the basis of the onset shift from 777 to 749 nm for a photovoltage of 50 mV, one can calculate a maximum conduction band shift of 60 mV. As shown in Figure 2, under white light illumination, similar increment of the open circuits photovoltage resulted from the TiO_2 coating by $SrTiO_3$.

The results presented above show that, in contrast to Nb_2O_5, the $SrTiO_3$ coating of the nanoporous TiO_2 electrode results in a negative shift of the TiO_2 bands rather than a formation of an energy barrier at its surface. The difference between the two systems can be related to one of the following structural issues: (i) the thickness of the coating layer and (ii) the coat continuity. On the basis of successive XPS measurements across the nanoporous film (utilizing the peel off methods reported in ref 21), we found that in both cases the coating material is present throughout the electrode. However, the quantities are quite different. Assuming uniform coating and that the particles are spherical and mono-sized, the thickness of the Nb_2O_5 layer is calculated to be over 2 nm, whereas the $SrTiO_3$ layer thickness is ca. 0.7 nm. The other way of presenting the XPS data would be partial coverage of a thick $SrTiO_3$ layer. In the case of thinner uniform coating of the $SrTiO_3$ compared with the Nb_2O_5 case, the absence of an energy barrier is related to the nature of the $SrTiO_3$ layer. The calculated $SrTiO_3$ layer thickness is close to the width of a single unit cell and thus the layer properties are not expected to be similar to those of bulk material. In other words, it is suggested that the conduction band potential of this thin $SrTiO_3$ layer is not higher than that of the TiO_2. Following this approach, the bands shift is related to the different electron affinity of $SrTiO_3$ and TiO_2, 3.7 and 4.3, respectively (the only available data relates to bulk material).[35] The difference in electron affinity forms a potential step at the TiO_2 surface which resembles the effect of a dipole layer. Recently, we showed that the latter induces a shift of the conduction band depending on the dipole direction and intensity.[31] The lower electron affinity value of the $SrTiO_3$ fits a negative shift of the TiO_2 bands.

The second approach relates to the continuity of the layer. Here the absence of an energy barrier is related to the recombination path through the noncoated area. The bands shift is again attributed to the formation of a potential step at the TiO_2 surface only that in this case it seems more reasonable to relate the step to the isoelectric point of TiO_2 and $SrTiO_3$. The isoelectric point of $SrTiO_3$, 7.8, is higher than that of TiO_2, 5.[36] Consequently, in solution, the $SrTiO_3$ is more positive than the TiO_2 which resembles the dipole layer pointing at the TiO_2.

At this point, we cannot predict which of the two mechanisms is relevant to the $SrTiO_3/TiO_2$ system. Further investigation in this direction that involves other materials coating is expected to reveal this issue.

Conclusions

The $SrTiO_3$ coating shifts the conduction band of the nanoporous TiO_2 electrode in the negative direction as a consequence of surface dipole generated at the $TiO_2/SrTiO_3$ interface. The surface dipole is a result of a difference in either the electron affinity or isoelectric point of the two semiconductors. It seems that the shifting mechanism can be related to the $SrTiO_3$ coverage; the electron affinity argument in the case of full coverage and the isoelectric point approach in the case of partial coverage.

When the $SrTiO_3$ coated TiO_2 electrode is applied in a DSSC, the open circuit photovoltage increases, while the short circuit photocurrent reduces resulting in an improvement of the overall conversion efficiency by 15.3%.

Acknowledgment. The authors thank the Israel Ministry of Science (MOS) for the support of this work. This work was done at the Bar-Ilan University as part of a Ph.D. thesis.

References and Notes

(1) O'Regan, B.; Gratzel, M. *Nature* **1991**, *353*, 737.
(2) Barbe, C. J.; Arendse, F.; Comte, P.; Jirousek, M.; Lenzmann, F.; Shklover, V.; Gratzel, M. *J. Am. Ceram. Soc.* **1997**, *80*, 3157.
(3) Parkinson, B. A.; Spitler, M. T. *Electrochim. Acta* **1992**, *37*, 943.
(4) Hagfeldt, A.; Gratzel, M. *Chem. Rev.* **1995**, *95*, 49.
(5) Bonhote, P.; Moser, J. E.; Vlachopoulos, N.; Walder, L.; Zakiruddin, S. M.; Humphry-Baker, R.; Pechy, P.; Gratzel, M. *Chem. Commun.* **1996**, 10.
(6) Argazzi, R.; Bignozzi, C. A.; Heimer, T. A.; Meyer, G. J. *Inorg. Chem.* **1997**, *36*, 2.
(7) Nazeeruddin, M. K.; Pechy, P.; Renouard, T.; Zakeeruddin, S. M.; Humphry-Baker, R.; Comte, P.; Liska, P.; Cevey, L.; Costa, E.; Shklover, V.; Spiccia, L.; Deacon, G. B.; Bignozzi, C. A.; Gratzel, M. *J. Am. Chem. Soc.* **2001**, *123*, 1613.
(8) Hagfeldt, A.; Lindquist, S. E.; Gratzel, M. *Sol. Energy Mater. Sol. Cells* **1994**, *32*, 245.
(9) Kavan, L.; Gratzel, M.; Gilbert, S. E.; Klemenz, C.; Scheel, H. J. *J. Am. Chem. Soc.* **1996**, *118*, 6716.
(10) Bisquert, J.; Garcia-Belmonte, G.; Fabregat-Santiago, F. *J. Solid State Electrochem.* **1999**, *3*, 337.
(11) Tachibana, Y.; Moser, J. E.; Gratzel, M.; Klug, D.; Durrant, J. R. *J. Phys. Chem.* **1996**, *100*, 20056.
(12) Kay, A.; Gratzel, M. *Chem. Mater.* **2002**, *14*, 2930.
(13) Kumara, G.; Tennakone, K.; Perera, V. P. S.; Konno, A.; Kaneko, S.; Okuya, M. *J. Phys. D Appl. Phys.* **2001**, *34*, 868.
(14) Tennakone, K.; Bandara, J.; Bandaranayake, P. K. M.; Kumara, G. R. A.; Konno, A. *Jpn. J. Appl. Phys. Pt. 2* **2001**, *40*, L732.
(15) Tennakone, K.; Perera, V. P. S.; Kottegoda, I. R. M.; De Silva, L. A. A.; Kumara, G.; Konno, A. *J. Electron. Mater.* **2001**, *30*, 992.
(16) Gregg, B. A.; Pichot, F.; Ferrere, S.; Fields, C. L. *J. Phys. Chem. B* **2001**, *105*, 1422.
(17) Kennedy, R.; Martini, I.; Hartland, G.; Kamat, P. V. *Proc. Indian Acad. Sci. Chem. Sci.* **1997**, *109*, 497.
(18) Nasr, C.; Kamat, P. V.; Hotchandani, S. *J. Phys. Chem. B* **1998**, *102*, 10047.
(19) Sant, P. A.; Kamat, P. V. *Phys. Chem. Chem. Phys.* **2002**, *4*, 198.
(20) Bedja, I.; Kamat, P. V. *J. Phys. Chem.* **1995**, *99*, 9182.
(21) Chappel, S.; Chen, S. G.; Zaban, A. *Langmuir* **2002**, *18*, 3336.
(22) Chen, S. G.; Chappel, S.; Diamant, Y.; Zaban, A. *Chem. Mater.* **2001**, *13*, 4629.
(23) Kumara, G. R. A.; Konno, A.; Tennakone, K. *Chem. Lett.* **2001**, 180.
(24) Tada, H.; Hattori, A. *J. Phys. Chem. B* **2000**, *104*, 4585.
(25) Tennakone, K.; Senadeera, G. K. R.; Perera, V. P. S.; Kottegoda, I. R. M.; De Silva, L. A. A. *Chem. Mater.* **1999**, *11*, 2474.
(26) Zaban, A.; Chen, S. G.; Chappel, S.; Gregg, B. A. *Chem. Commun.* **2000**, 2231.
(27) Burnside, S.; Moser, J. E.; Brooks, K.; Gratzel, M.; Cahen, D. *J. Phys. Chem. B* **1999**, *103*, 9328.
(28) Lenzmann, F.; Krueger, J.; Burnside, S.; Brooks, K.; Gratzel, M.; Gal, D.; Ruhle, S.; Cahen, D. *J. Phys. Chem. B* **2001**, *105*, 6347.
(29) Kruger, J.; Bach, U.; Gratzel, M. *Adv. Mater.* **2000**, *12*, 447.
(30) Vilan, A.; Shanzer, A.; Cahen, D. *Nature* **2000**, *404*, 166.
(31) Zaban, A.; Chen, S. G.; Sukenik, C. N.; Pizem, H. *Abstr. Paper Am. Chem. Soc.* **2001**, *222*, 285.
(32) Liu, C. Y.; Bard, A. J. *J. Phys. Chem.* **1989**, *93*, 3232.
(33) Fitzmaurice, D. *Sol. Energy Mater. Sol. Cells* **1994**, *32*, 289.
(34) Zaban, A.; Meier, A.; Gregg, B. A. *J. Phys. Chem. B* **1997**, *101*, 7985.
(35) Rienstra-Kiracofe, J. C.; Tschumper, G. S.; Schaefer, H. F.; Nandi, S.; Ellison, G. B. *Chem. Rev.* **2002**, *102*, 231.
(36) Parks, G. A. *The Isoelectric Points of Solids Oxides, Solid Hydroxides, and Aqueous Hydroxo Complex Systems*; Department of Mineral Engineering: Stanford University, Stanford, California, 1964.